

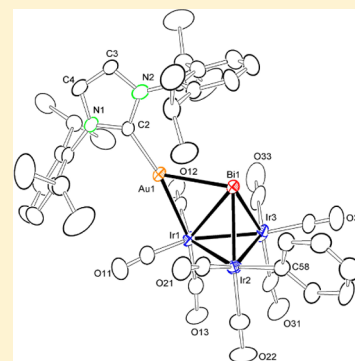
The Addition of Gold and Tin to Bismuth–Triiridium Carbonyl Complexes

Richard D. Adams* and Gaya Elpitiya

Department of Chemistry and Biochemistry, University of South Carolina, Columbia, South Carolina 29208, United States

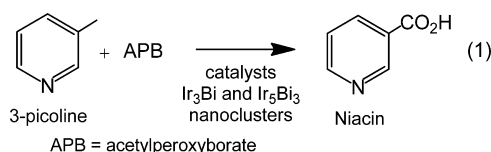
S Supporting Information

ABSTRACT: The reaction of $\text{Ir}_3(\text{CO})_9(\mu_3\text{-Bi})$ with $\text{PhAu}(\text{NHC})$ (1), where $\text{NHC} = 1,3\text{-bis}(2,6\text{-diisopropylphenylimidazol-2-ylidene})$, has yielded the compound $\text{Ir}_3(\text{CO})_8(\text{Ph})-(\mu_3\text{-Bi})[\mu\text{-Au}(\text{NHC})]$ (2) by the loss of one CO ligand and the oxidative addition of the Au–C (phenyl) bond of 1 to one of the iridium atoms. The $\text{Au}(\text{NHC})$ group bridges one of the Ir–Bi bonds of the cluster. On the basis of X-ray crystal structural analysis and molecular orbital and quantum theory of atoms in molecules calculations, the Au–Bi interaction was determined to be substantial and is comparable in character to the Ir–Bi and Ir–Ir bonds in this cluster. Compound 2 reacts with 2 equiv of HSnPh_3 to yield the compound $\text{Ir}_3(\text{CO})_7(\text{SnPh}_3)_2(\mu_3\text{-Bi})[\mu\text{-Au}(\text{NHC})](\mu\text{-H})$ (3), which contains two terminally coordinated SnPh_3 ligands. Compound 3 reacts with H_2O to yield the compound $\text{Ir}_3(\mu_3\text{-Bi})(\text{CO})_7[\mu\text{-Ph}_2\text{Sn}(\text{OH})\text{SnPh}_2][\mu\text{-Au}(\text{NHC})]$ (4) by cleavage of a phenyl ring from each of the SnPh_3 ligands and formation of a bridging OH group between the two tin atoms to form a chelating $\text{Ph}_2\text{Sn}(\text{OH})\text{SnPh}_2$ ligand.



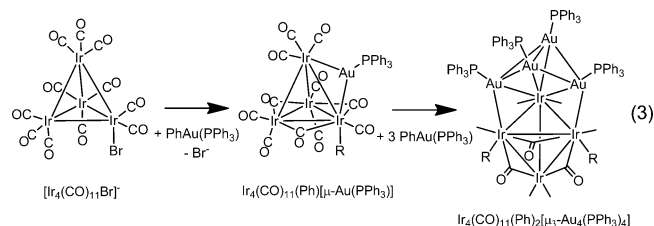
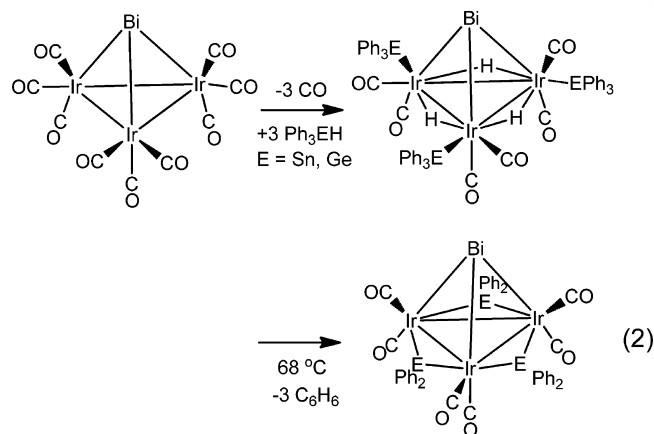
INTRODUCTION

Bismuth has been found to exhibit valuable properties as a catalyst and cocatalyst for the selective oxidation and ammoxidation of hydrocarbons.¹ We have recently shown that iridium–bismuth nanoparticles derived from bimetallic iridium–bismuth carbonyl complexes exhibit good activity for the direct conversion of 3-picoline to niacin at 65 °C by using acetylperoxyborate as the oxidant (eq 1).² Gold clusters and



nanoparticles have recently been shown to exhibit remarkable activity for the selective oxidation of certain hydrocarbons.³ Tin is also well-known to be a modifier of heterogeneous transition-metal catalysts.⁴ We have already shown that HSnPh_3 and HGePh_3 can be added to $\text{Ir}_3(\text{CO})_9(\mu_3\text{-Bi})$ to yield products containing terminal EPh_3 ligands, $\text{Ir}_3(\text{CO})_6(\text{EPh}_3)_3(\mu_3\text{-Bi})(\mu\text{-H})_3$, $\text{E} = \text{Sn}$ and Ge , and bridging EPh_2 ligands, $\text{Ir}_3(\text{CO})_6(\mu\text{-EPh}_2)_3(\mu_3\text{-Bi})$, $\text{E} = \text{Sn}$ and Ge (eq 2).⁵ We have recently shown the molecule $\text{PhAu}(\text{PPh}_3)$ can be oxidatively added to substitutionally active metal carbonyl cluster complexes under mild conditions to yield transition metal–gold complexes containing phenyl ligand(s), e.g., eqs 3–5.^{6–8}

With this in mind, we have now embarked on a study to synthesize new iridium–bismuth complexes derived from $\text{Ir}_3(\text{CO})_9(\mu_3\text{-Bi})$ that contain gold and gold plus tin ligands that could potentially be converted into new multimetallic nanoparticles for applications in selective oxidation catalysis. The results of these studies are reported herein.



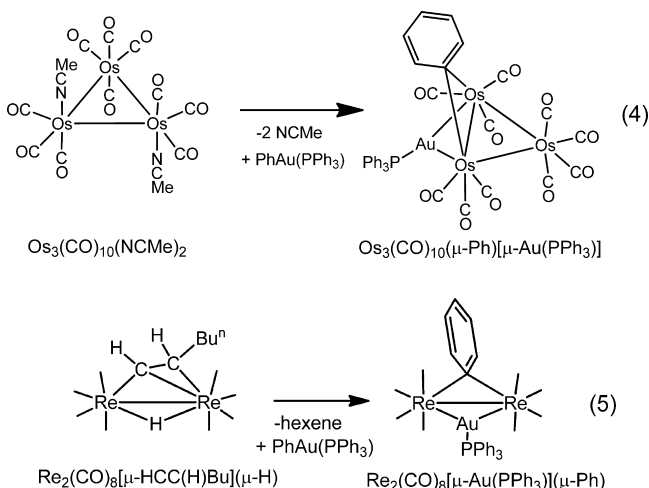
EXPERIMENTAL SECTION

General Data. Reagent-grade solvents were dried by the standard procedures and freshly distilled prior to use. All reactions were performed under an atmosphere of nitrogen unless indicated otherwise. IR spectra were recorded on a Thermo Nicolet Avatar 360 FT-IR

Received: June 4, 2015

Published: August 6, 2015





spectrophotometer. Room temperature ^1H NMR spectra were recorded on a Varian Mercury 300 spectrometer operating at 300.1 MHz. Variable-temperature ^1H NMR spectra were recorded on a Varian Mercury 400 spectrometer operating at 161.9 MHz. Positive/negative-ion mass spectra were recorded on a Micromass Q 2 -TOF instrument by using electrospray (ES) ionization. $\text{Ir}_4(\text{CO})_{12}$, $\text{ClAu}(\text{NHC})$, where NHC = 1,3-bis(2,6-diisopropylphenyl)imidazol-2-ylidene, and $\text{Bi}(\text{NO}_3)_3 \cdot 5\text{H}_2\text{O}$ were obtained from STREM and used without further purification. Ph_3SnH was obtained from Aldrich and used without further purification. $\text{PhAu}(\text{NHC})$ (**1**) was prepared from $\text{ClAu}(\text{NHC})$ by a slightly modified version of the reported procedure for $\text{PhAu}(\text{PPh}_3)$; see below.⁹ $[\text{PPN}]\text{Ir}(\text{CO})_4$ was prepared according to the previously reported procedure.¹⁰ $\text{Ir}_3(\text{CO})_9(\mu_3\text{-Bi})$ was prepared by a modified procedure, according to the previous reports.^{5,11} Product separations were performed by thin-layer chromatography (TLC) in air on Analtech 0.25 mm silica gel 60 Å F254 and 0.25 mm aluminum oxide 60 Å F254 glass plates.

Synthesis of 1,3-Bis(2,6-diisopropylphenyl)imidazol-2-ylidenegold(I) Phenyl (1). In dry isopropyl alcohol (10 mL), phenylboronic acid (56.94 mg, 0.467 mmol) was dissolved and Cs_2CO_3 (146.89 mg, 0.451 mmol) was added. To this suspension was added $\text{ClAu}(\text{NHC})$ (150.0 mg, 0.241 mmol) under nitrogen, and the resultant mixture was stirred at 50 °C for 24 h. The solvent was then removed in vacuo, and the solid was extracted with benzene, filtered through Celite, and concentrated in vacuo to dryness. This yielded 155.0 mg of the colorless product **1** (97% yield). The ^1H NMR spectrum of **1** was identical with that reported in the original work.¹²

Synthesis of $\text{Ir}_3(\text{CO})_8(\text{Ph})(\mu_3\text{-Bi})[\mu\text{-Au}(\text{NHC})]$ (2). A 39.3 mg (0.063 mmol) portion of **1** was added to 24.6 mg (0.021 mmol) of $\text{Ir}_3(\text{CO})_9(\mu_3\text{-Bi})$, which was dissolved in 30 mL of hexane. The reaction was heated to reflux for 45 min. The solvent was then removed in vacuo, and the product was isolated by TLC with a 6:1 hexane/methylene chloride solvent ratio as the eluent. This gave 14.6 mg (0.009 mmol) of red **2** or 42% yield. Spectral data for **2**: IR (cm^{-1} in CH_2Cl_2) $\nu(\text{CO})$ 2065(m), 2037(vs), 2010 (s), 2003 (s); ^1H NMR (CD_2Cl_2 , δ in ppm) 7.55 (t, $^3J_{\text{H-H}} = 6$ Hz, 2H, *p*-CH), 7.37 (d, $^3J_{\text{H-H}} = 9$ Hz, 4H, *m*-CH), 7.31 (s, 2H, *NCH}_2), 2.63 (sept, $^3J_{\text{H-H}} = 6$ Hz, 4H, $\text{CH}(\text{CH}_3)_2$), 1.33 (d, $^3J = 9$ Hz, 12H, $\text{CHC}(\text{CH}_3)_2$), 1.22 (d, $^3J_{\text{H-H}} = 6$ Hz, 12H, $\text{CHC}(\text{CH}_3)_2$), 6.68–7.22 (m, 5H, σ -Ph); MS ES (negative ion) for **2** m/z 1785 [(M + triflate) $^-$]; MS ES (positive ion) for **2** m/z 1672 (M^+). The isotope distribution pattern is consistent with the presence of three iridium atoms, one bismuth atom, and a gold atom.*

Synthesis of $\text{Ir}_3(\text{CO})_7(\text{SnPh}_3)_2(\mu_3\text{-Bi})[\mu\text{-Au}(\text{NHC})](\mu\text{-H})$ (3). A 42.3 mg (0.025 mmol) portion of **2** dissolved in 20 mL of CH_2Cl_2 was stirred with 68.0 mg (0.192 mmol) of HSnPh_3 for 1 h at room temperature. The solvent was then removed in vacuo, and the product was isolated by TLC on alumina using a 6:1 hexane/methylene chloride solvent mixture. This gave 13.1 mg (0.0060 mmol) of orange **3** or 24% yield. Spectral data for **3**: IR (cm^{-1} in CH_2Cl_2) $\nu(\text{CO})$ 2058(s), 2035(vs), 2018 (m), 2005 (s); ^1H NMR (CD_2Cl_2 , δ in ppm, at 25 °C) 7.8–6.92 (m, 36H, Ph), 2.57 (sept, $^3J_{\text{H-H}} = 6$ Hz, 4H, $\text{CH}(\text{CH}_3)_2$), –19.57 (s, br,

1H, Ir–H); at –80 °C, the hydride signal appears as two resonances at δ –18.00 (s, 1H, Ir–H, $^2J_{\text{Sn-H}} = 20$ Hz) and –21.69 (s, 1H, Ir–H, $^2J_{\text{Sn-H}} = 20$ Hz); MS ES (positive ion) for **3** m/z 2307 ($\text{M} + \text{K}^+$). The isotope distribution pattern is consistent with the presence of three iridium atoms, one bismuth atom, a gold atom, and two tin atoms.

Synthesis of $\text{Ir}_3(\mu_3\text{-Bi})(\text{CO})_7[\mu\text{-Ph}_2\text{Sn}(\text{OH})\text{SnPh}_2][\mu\text{-Au}(\text{NHC})]$ (4). A 7.8 mg (0.003 mmol) portion of **3** was dissolved in 4 mL of CD_2Cl_2 in an NMR tube. A total of 0.1 mL of H_2O was added, and the sample was heated to 40 °C for 3 h. The product was isolated by TLC on alumina using a 6:1 hexane/methylene chloride solvent mixture as the eluent. This gave 1.8 mg (0.0008 mmol) of orange **4** or 24% yield. Spectral data for **4**: IR (cm^{-1} in CH_2Cl_2) $\nu(\text{CO})$ 2043(s), 1993.99 (vs), 1948.54 (w); ^1H NMR (CD_2Cl_2 , δ in ppm) 7.8–6.88 (m, 26H, Ph), 2.62 (sept, $^3J_{\text{H-H}} = 6$ Hz, 4H, $\text{CH}(\text{CH}_3)_2$), 3.15 (s, OH, Sn–OH, $^2J_{\text{Sn-OH}} = 15$ Hz); MS ES (positive ion) for **4** m/z 2169 ($\text{M} + \text{K}^+$). The isotope distribution pattern is consistent with the presence of three iridium atoms, one bismuth atom, a gold atom, two tin atoms, and an OH.

Reaction of **2 with Ph_3SnH and H_2O .** A 27.4 mg (0.016 mmol) portion of **2** dissolved in 4 mL of CD_2Cl_2 in an NMR tube was mixed to react with 0.1 mL of H_2O and 17.4 mg (0.049 mmol) of HSnPh_3 for 24 h at 25 °C. The products were isolated by TLC on alumina using a 6:1 hexane/methylene chloride solvent mixture for elution. This gave 4.5 mg (0.002 mmol) of compound **3** (24% yield) and 2.2 mg (0.001 mmol) of compound **4** (13% yield).

Crystallographic Analyses. Red single crystals of **2** and orange single crystals of **3** and **4** suitable for X-ray diffraction analyses were obtained by slow evaporation of the solvent from a solution of the compound in hexane at room temperature. Each data crystal was glued onto the end of a thin glass fiber. X-ray intensity data were measured by using a Bruker SMART APEX CCD-based diffractometer with Mo $K\alpha$ radiation ($\lambda = 0.71073$ Å). The raw data frames were integrated with the SAINT+ program using a narrow-frame integration algorithm.¹³ Corrections for Lorentz and polarization effects were also applied with SAINT+. All structures were solved by a combination of direct methods and difference Fourier syntheses and refined by full-matrix least squares on F^2 using the SHELXTL software package.¹⁴ All non-hydrogen atoms were refined with anisotropic displacement parameters. Crystal data, data collection parameters, and the results of analyses are listed in Table S1 in the Supporting Information.

Computational Details. All density functional theory (DFT) calculations were performed with the Amsterdam Density Functional (ADF) suite of programs¹⁵ using the PBEsol functional¹⁶ with a valence quadruple- ζ + 4 polarization function, relativistically optimized basis sets for iridium, bismuth, and gold atoms, and double- ζ basis sets for carbon, oxygen, nitrogen, and hydrogen atoms with no frozen cores. The molecular orbitals and their energies were determined by a geometry-optimized (GO) calculation with scalar relativistic corrections that were initiated using the atom positional parameters as determined from crystal structure analyses. Electron densities at the bond critical points (bcps) were calculated by using the Bader quantum theory of atoms in molecules (QTAIM) model; see the Supporting Information.^{17,18}

RESULTS AND DISCUSSION

The reaction of **1** with $\text{Ir}_3(\text{CO})_9(\mu_3\text{-Bi})$ in a hexane solvent at reflux for 45 min yielded the new compound **2** in 42% yield. Compound **2** was characterized by a combination of IR and ^1H NMR spectroscopies, mass spectrometry, and a single-crystal X-ray diffraction analysis. An ORTEP diagram of the molecular structure of **2** is shown in Figure 1. Like its parent $\text{Ir}_3(\text{CO})_9(\mu_3\text{-Bi})$, compound **2** consists of a triangular cluster of three iridium atoms with a triply bridging bismuth atom. The Ir–Ir bond lengths in **2**, Ir1–Ir2 = 2.8115(3) Å, Ir1–Ir3 = 2.8150(3) Å, and Ir2–Ir3 = 2.7647(3) Å, are slightly longer than those in $\text{Ir}_3(\text{CO})_9(\mu_3\text{-Bi})$ [average 2.734(2) Å].¹¹ Compound **2** contains an $\text{Au}(\text{NHC})$ group that bridges one of the Ir–Bi bonds. The Ir–Au distance, Ir1–Au1 = 2.7165(3) Å, is similar to that found in the compound $\text{Ir}_4(\text{CO})_{11}(\text{Ph})[\mu\text{-AuPPh}_3]$, Ir1–Au1 = 2.7332(4) Å and Ir2–Au1 = 2.8056(4) Å.¹⁹ The Au–Bi bond distance in **2**,

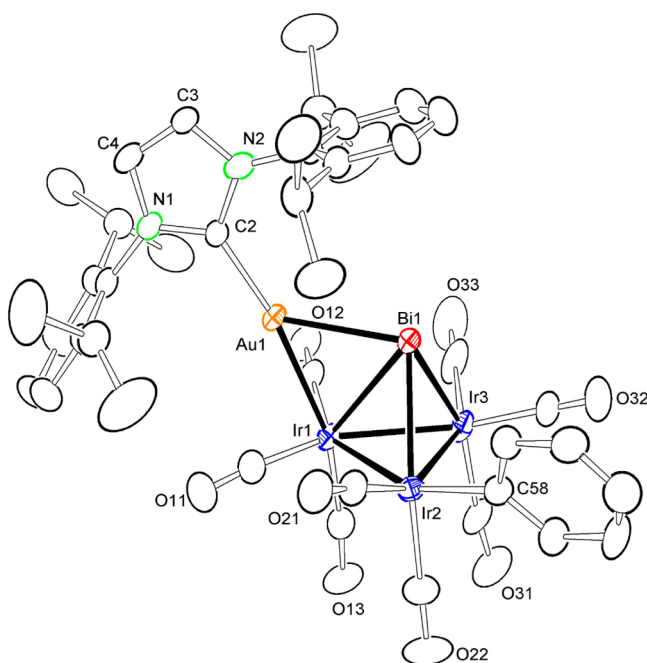


Figure 1. ORTEP diagram of the molecular structure of **2** showing 20% thermal ellipsoid probability. Hydrogen atoms are not shown for clarity. Selected interatomic bond distances (Å) and angles (deg) are as follows: Ir1–Au1 = 2.7165(3), Au1–Bi1 = 2.8189(3), Ir1–Bi1 = 2.9461(3), Ir2–Bi1 = 2.6738(3), Ir3–Bi1 = 2.7166(4), Ir1–Ir2 = 2.8115(3), Ir1–Ir3 = 2.8150(3), Ir2–Ir3 = 2.7647(3); Ir1–Au1–Bi1 = 64.281(8), Ir2–Bi1–Au1 = 101.342(10), Ir3–Bi1–Au1 = 111.587(11), Ir2–Bi1–Ir3 = 61.709(9), Ir2–Bi1–Ir1 = 59.804(8), Ir3–Bi1–Ir1 = 56.173(7), Ir1–Ir3–Ir2 = 60.507(8), Ir2–Ir1–Ir3 = 58.861(8), Ir1–Ir2–Ir3 = 60.632(8), Au1–Ir1–Ir2 = 100.469(10), Au1–Ir1–Ir3 = 111.707(11).

Au1–Bi1 = 2.8189(3) Å, is only slightly longer than the Ir–Au distance and appears to be the shortest observed to date. There are very few structural characterizations of complexes containing Au–Bi bonds with which to compare. Fernandez et al. reported the compound $[\text{Au}(\text{C}_6\text{F}_5)_2][\text{Bi}(\text{C}_6\text{H}_4\text{CH}_2\text{NMe}_2)_2]$, which contained a very long Au⋯Bi interaction, 3.7284(5) Å, that was more ionic in character than covalent.²⁰ The pincer complex $[o\text{-(Ph}_2\text{P)}\text{C}_6\text{H}_4]_2\text{BiClAuCl}$ contains a decidedly more covalent

Au–Bi interaction, and the Au–Bi distance in **2** is much shorter, 2.9738(17)²¹ and 2.9979(3) Å.²² The Ir–Bi distances in **2**, Ir1–Bi1 = 2.9461(3) Å, Ir2–Bi1 = 2.6738(3) Å, and Ir3–Bi1 = 2.7166(4) Å, are similar to those in $\text{Ir}_3(\text{CO})_9(\mu_3\text{-Bi})$ [average 2.734(2) Å], except for the gold-bridged Ir–Bi bond Ir1–Bi1, which is considerably longer. There is a terminally coordinated phenyl ligand bonded to Ir2, Ir2–C58 = 2.090(7) Å, which has a Ir–C distance similar to that of the phenyl ligand found in the tetrairidium compounds $\text{Ir}_4(\text{CO})_{11}(\text{Ph})[\mu\text{-Au}(\text{PPh}_3)]$, Ir–C = 2.100(7) Å,¹⁹ and $[\text{Ir}_4(\text{CO})_{11}\text{Ph}]^-$, Ir–C = 2.125(13) Å.²³ One of the aryl rings from the carbene ligand is positioned over the bismuth atom. The distance between the bismuth atom and the centroid of this ring is 3.892 Å. Arenes are known to form π complexes to bismuth over a range of distances.²⁴ Bismuth to ring centroid distances in the range of 3.0–3.2 Å are generally regarded as fairly strong acid–base interactions.²⁵ There is evidence that Bi– π -arene interactions are important to crystal packing for certain organobismuth solid-state structures.^{24–26}

In order to gain some understanding of the bonding of the gold atom to the bismuth atom in **2**, a DFT molecular orbital analysis was performed using the PBEsol functional of the ADF program library. Selected molecular orbitals for **2** are shown in Figure 2. The bonding of the bismuth atom to the triiridium cluster is represented in HOMO, HOMO–1, and HOMO–2. These molecular orbitals are principally Bi–Ir cluster bonding. Au–Ir bonding is shown in HOMO–7, and Au–Bi bonding is shown in HOMO–10. The Au–Bi bond is composed principally of the 6s orbital on gold and the 6p_z orbital on bismuth in the coordinate system shown in Figure 2. In order to analyze the Au–Bi bonding further, we have calculated the electron densities at the bcps for a number of heavy atom pairs using the Bader QTAIM model.^{17,18} A plot of **2** that shows the locations of the various bcps is shown in Figure 3, and a listing of the GO bond distances with their electron densities (e^-/bohr^3) at the bcps is given in Table 1. The GO DFT Au–Bi bond distance is slightly longer, 2.8674 Å, than the experimental value, Au1–Bi1 = 2.8189(3) Å. The DFT calculation may be slightly underestimating the strength of the Au–Bi bond. Nevertheless, the QTAIM electron density at the Au–Bi bcp, 0.04756 e^-/bohr^3 , is only slightly smaller than that of the Ir–Au bond, 0.05902 e^-/bohr^3 ; the electron density at Ir–Bi bcps range from 0.05382 to 0.06665 e^-/bohr^3 , and those of the Ir–Ir bonds range from 0.05463 to 0.05621 e^-/bohr^3 .

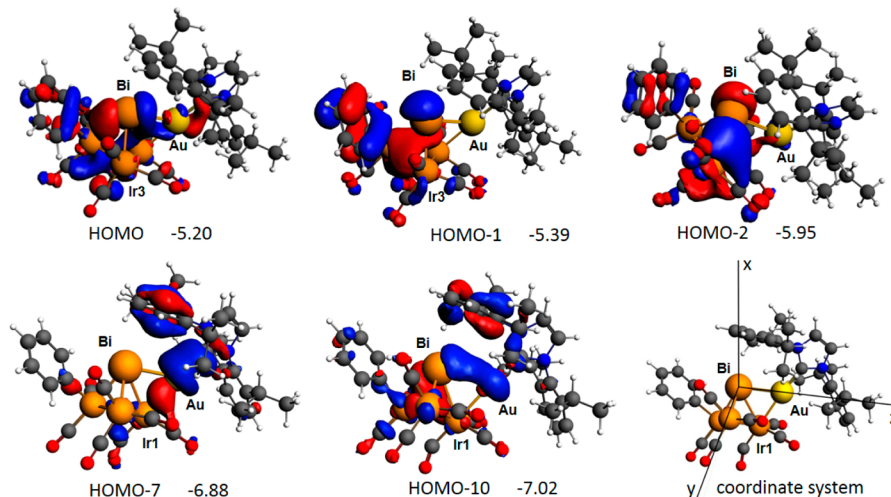


Figure 2. Selected GO DFT molecular orbitals for compound **2** with corresponding energies in electronvolts (eV) and a view showing the orientation of the applied coordinate system. The isovalue is 0.03. The Bi–Au bond is the z axis in the coordinate system.

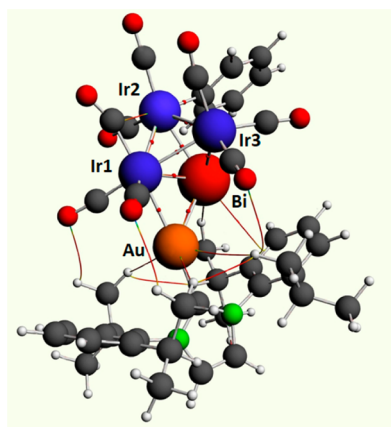


Figure 3. Plot of the GO DFT structure of **2** showing the locations of selected bcps in red.

Table 1. GO DFT-Calculated Bond Distances (Å) with Corresponding QTAIM Electron Densities (e^-/bohr^3) at the bcps for Compound **2**

atom 1	atom 2	bond distance	electron density at bcp
Au	Bi	2.8674	0.04756
Au	Ir1	2.6862	0.05902
Bi	Ir1	2.8681	0.05382
Bi	Ir2	2.7348	0.06665
Bi	Ir3	2.7589	0.06181
Ir1	Ir2	2.7750	0.05463
Ir1	Ir3	2.7610	0.05621
Ir2	Ir3	2.7825	0.05498

The iridium atoms in compound **2** contain a total of 48 cluster valence electrons, and with three Ir–Ir bonds, the complex

is formally electron-precise; i.e., all of the iridium atoms have 18-electron configurations.

Next, the reaction of **2** with HSnPh_3 was investigated. The reaction of **2** with HSnPh_3 at room temperature for 1 h yielded the new compound **3** in 24% yield. Compound **3** was characterized by a combination of IR and ^1H NMR spectroscopies, mass spectrometry, and single-crystal X-ray diffraction analysis. An ORTEP diagram of the molecular structure of **3** is shown in Figure 4. Compound **3** contains a bismuth-bridged triiridium triangle with an $\text{Au}(\text{NHC})$ group that bridges one of the Ir–Bi bonds, which is similar to that observed in **2**. In addition, compound **3** contains two SnPh_3 ligands that occupy equatorial coordination sites, one on each of the two $\text{Ir}(\text{CO})_2$ groups. The Ir–Sn bond distances are similar in length, $\text{Ir3–Sn1} = 2.6415(18)$ Å, $\text{Ir2–Sn2} = 2.6413(19)$ Å, and are similar to those found in the compounds $\text{Ir}_3(\text{CO})_6(\text{SnPh}_3)_3(\mu\text{-H})_3(\mu_3\text{-Bi})^5$ and $\text{Ir}_3(\text{CO})_6(\text{SnPh}_3)_3(\mu\text{-SnPh}_2)_3$.²⁷ There is a hydride ligand bridging the Ir–Ir bond between the two tin-substituted iridium atoms. At room temperature, the ^1H NMR resonance of the hydrido ligand was observed at $\delta -19.57$, but the signal was very broad. Because dynamical activity was suspected, variable-temperature ^1H NMR spectra of **2** were obtained. At -80 °C, the hydride signal for **2** appears as two sharp resonances at $\delta -18.00$ (s, $^2J_{\text{Sn–H}} = 20$ Hz) and $\delta -21.69$ (s, $^2J_{\text{Sn–H}} = 20$ Hz) with relative intensities of 0.4 and 0.6. These resonances broaden and coalesce at $\delta -19.57$ as the temperature is raised to 25 °C. This observation can be explained by the presence of two coordination isomers of **2** in solution that interconvert rapidly on the NMR time scale at 25 °C. Similar dynamical activity was observed for the very similar compound $\text{Ir}_3(\text{CO})_6(\text{GePh}_3)_3(\mu\text{-H})_3(\mu_3\text{-Bi})$.⁵ The Ir–Ir bond distances in **3** are similar to those found in **2**, $\text{Ir1–Ir3} = 2.8211(14)$ Å and $\text{Ir1–Ir2} = 2.8221(13)$ Å, except for the hydride-bridged Ir–Ir bond, $\text{Ir2–Ir3} = 2.9098(14)$ Å,

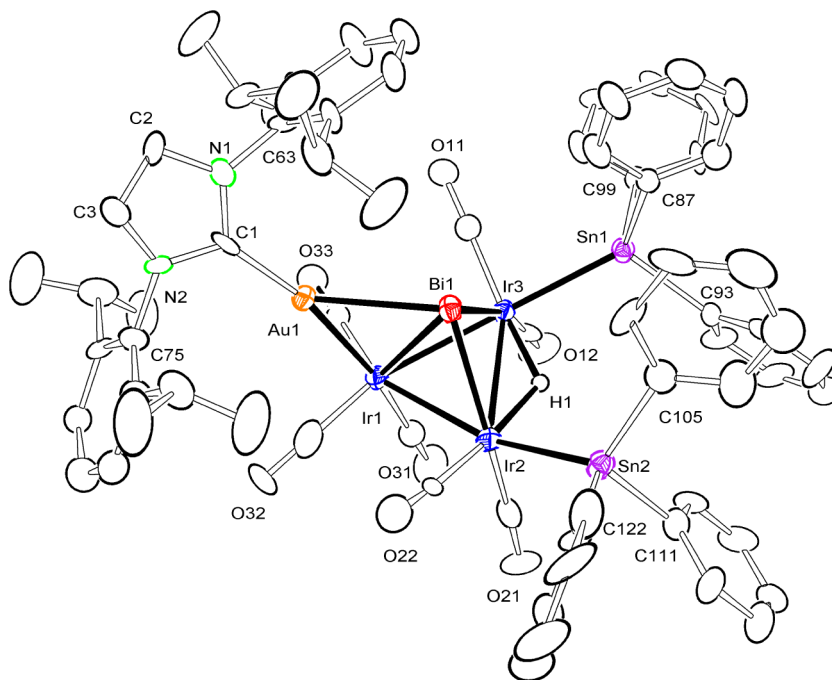


Figure 4. ORTEP diagram of the molecular structure of **3** showing 20% thermal ellipsoid probability. Selected interatomic bond distances (Å) and angles (deg) are as follows: $\text{Ir1–Ir3} = 2.8211(14)$, $\text{Ir1–Ir2} = 2.8221(13)$, $\text{Ir2–Ir3} = 2.9098(14)$, $\text{Ir2–H1} = 1.699(10)$, $\text{Ir3–H1} = 1.696(10)$, $\text{Ir1–Bi1} = 2.9919(13)$, $\text{Ir3–Bi1} = 2.7125(12)$, $\text{Ir2–Bi1} = 2.6937(14)$, $\text{Au1–Bi1} = 2.8295(13)$, $\text{Ir3–Sn1} = 2.6415(18)$, $\text{Ir2–Sn2} = 2.6413(19)$; $\text{Ir1–Au1–Bi1} = 65.39(3)$, $\text{Ir3–Bi1–Ir1} = 59.04(3)$, $\text{Ir2–Bi1–Ir1} = 59.24(3)$, $\text{Ir2–Bi1–Ir3} = 65.13(3)$, $\text{Ir1–Ir3–Ir2} = 58.98(3)$, $\text{Ir1–Ir2–Ir3} = 58.94(3)$, $\text{Ir3–Ir1–Ir2} = 62.08(3)$, $\text{Ir2–Bi1–Au1} = 106.41(4)$, $\text{Ir3–Bi1–Au1} = 103.42(4)$.

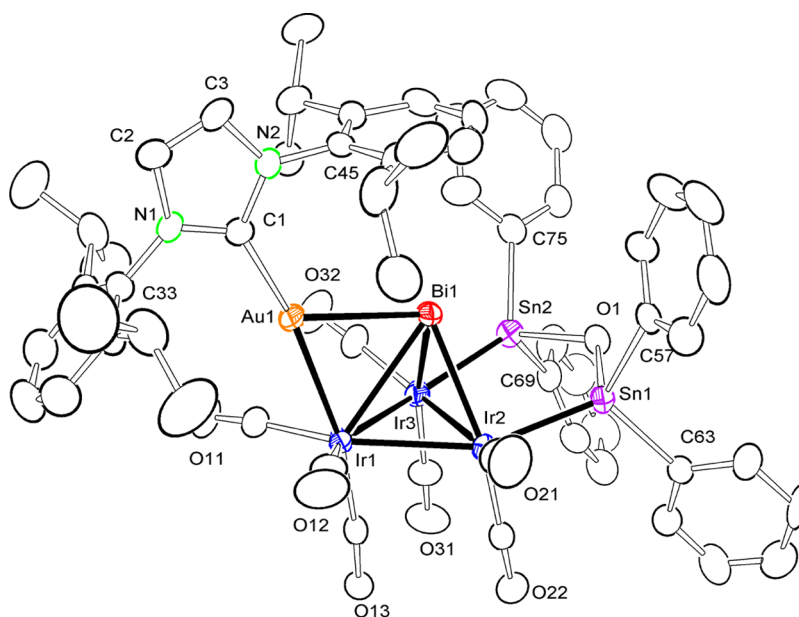


Figure 5. ORTEP diagram of the molecular structure of **4** showing 20% thermal ellipsoid probability. Hydrogen atoms are not shown for clarity. Selected interatomic bond distances (Å) and angles (deg) are as follows: Au1–Ir1 = 2.7080(6), Au1–Bi1 = 2.8703(6), Bi1–Ir3 = 2.6979(6), Bi1–Ir2 = 2.7036(6), Bi1–Ir1 = 2.9406(6), Ir2–Sn1 = 2.5505(9), Ir2–Ir3 = 2.7736(7), Ir2–Ir1 = 2.8082(7), Ir3–Sn2 = 2.5565(10), Ir3–Ir1 = 2.8087(7), O1–Sn1 = 2.118(8), O1–Sn2 = 2.143(8); Ir1–Au1–Bi1 = 63.547(16), Ir2–Ir3–Ir1 = 60.401(18), Ir3–Ir2–Ir1 = 60.418(18), Ir2–Ir1–Ir3 = 59.181(17), Ir2–Bi1–Ir1 = 59.498(16), Ir3–Bi1–Ir1 = 59.567(17), Ir3–Bi1–Ir2 = 61.792(18), Sn1–O1–Sn2 = 121.2(4).

which is elongated because of the presence of the hydride ligand.²⁸ The Ir–Bi distances are similar to those found in **2**, Ir1–Bi1 = 2.9919(13) Å, Ir3–Bi1 = 2.7125(12) Å, and Ir2–Bi1 = 2.6937(14) Å, and the gold-bridged Ir–Bi bond, Ir1–Bi1, is significantly longer than the unbridged Ir–Bi bonds. Compound **3** contains also an Au–Bi bond that is similar in length to that found on **2**, Au1–Bi1 = 2.8295(13) Å. The iridium atoms in compound **3** contain a total of 48 cluster valence electrons, and with three Ir–Ir bonds, the complex is formally electron-precise.

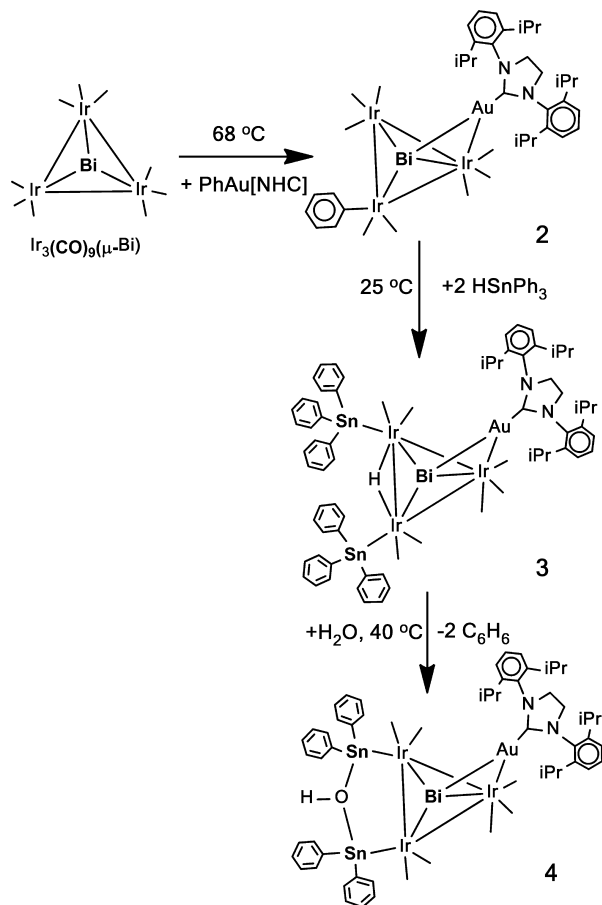
When compound **2** was allowed to react with HSnPh₃ in the presence of H₂O for 24 h at 25 °C, compound **3** was obtained in 24% yield, together with the new compound **4** in 13% yield. It was subsequently shown that compound **4** can be obtained in an even better yield (24%) directly by the reaction of **3** with H₂O. Compound **4** was characterized by a combination of IR and ¹H NMR spectroscopies, mass spectrometry, and single-crystal X-ray diffraction analysis. An ORTEP diagram of the molecular structure of **4** is shown in Figure 5. Compound **4** contains an AuBiIr₃ cluster of metal atoms that is similar to that in compounds **2** and **3**. The bismuth atom is bonded to all three iridium atoms, and an Au(NHC) group bridges one of the Ir–Bi bonds. As in **2** and **3**, the Au(NHC)-bridged Ir–Bi bond, Bi1–Ir1, is substantially longer than the unbridged Ir–Bi bonds, Bi1–Ir1 = 2.9406(6) Å, Bi1–Ir3 = 2.6979(6) Å, and Bi1–Ir2 = 2.7036(6) Å. The Ir–Ir bond distances, Ir1–Ir2 = 2.8082(7) Å, Ir1–Ir3 = 2.8087(7) Å, and Ir2–Ir3 = 2.7736(7) Å, are similar to those in **2**. The most interesting ligand in **4** is a Ph₂Sn(OH)SnPh₂ group that bridges the Ir2–Ir3 bond of the cluster as a chelating ligand; one tin atom is bonded to each of the two iridium atoms. The Ir–Sn distances, Ir2–Sn1 = 2.5505(9) Å and Ir3–Sn2 = 2.5565(10) Å, are significantly shorter (approximately 0.09 Å) than the Ir–Sn distances in **3**. An OH group bridges the two tin atoms, O1–Sn1 = 2.118(8) Å and O1–Sn2 = 2.143(8) Å. The hydrogen atom on the oxygen atom O1 was not located in this structural analysis but was detected in the ¹H NMR spectrum of **4** at δ 3.15

(²J_{Sn–OH} = 15 Hz). Bridging Ph₂Sn(OH)SnPh₂ ligands are rare, but one was observed and structurally characterized previously in the compound [Mn₂(CO)₆(μ-H){μ-Ph₂Sn(OH)SnPh₂}-[μ-(EtO)₂POP(OEt)₂]: Sn–O = 2.12(1) Å, which was obtained from the reaction of [Mn₂(CO)₆(μ-H)₂(μ-(EtO)₂POP(OEt)₂)] with HSnPh₃; the oxygen atom between the tin atoms was suspected of being derived from traces of H₂O in the reaction mixture.²⁹ The reaction of Re₂(CO)₈[μ-C(H)C(H)Buⁿ](μ-H) with HGePh₃ in the presence of H₂O yielded the compound Re₂(CO)₈[μ-Ph₂Ge(OH)GePh₂](μ-H) containing a bridging Ph₂Ge(OH)GePh₂ ligand, and the addition of OMe[−] to Re₂(CO)₈(μ-SnPh₂)₂ yielded the anionic compound Re₂(CO)₈[μ-Ph₂Sn(OMe)SnPh₂][−] containing a bridging Ph₂Sn(OMe)SnPh₂ ligand.³⁰ Although the molecule has no charge overall, the Ph₂Sn(OH)SnPh₂ ligand in **4** does have a formal charge of 1+ located on the trivalent oxygen atom. Overall, the Ph₂Sn(OH)SnPh₂ ligand would serve as a two-electron donor to the cluster; thus, the three iridium atoms would have a total of 48 cluster valence electrons, and with three Ir–Ir bonds, each of the iridium atoms would formally have an 18-electron configuration.

SUMMARY AND CONCLUSIONS

A summary of the reactions studied in this work is shown in Scheme 1. Ir₃(CO)₉(μ₃-Bi) was found to react with PhAu(NHC) by losing one CO ligand, and the Au–C bond to the phenyl ligand was added to one of the iridium atoms to yield compound **2**, which contains a σ-coordinated phenyl ligand on an iridium atom and an Au(NHC) group bridging one of the Ir–Bi bonds of the cluster. Assuming that gold is more electronegative than iridium, this addition is formally an “oxidative addition”, although the mechanism of the process has not been established in this study. On the basis of the structural analysis and the molecular orbital and QTAIM calculations, the Au–Bi interaction is substantial and is comparable in character to the Ir–Bi and Ir–Ir bonds in this cluster. We have shown previously that Ir₃(CO)₉(μ₃-Bi) reacts with HSnPh₃ by adding 3 equiv of HSnPh₃

Scheme 1. Summary of the Work Done in This Report



to yield the compound $\text{Ir}_3(\text{CO})_6(\text{SnPh}_3)_3(\mu_3\text{-Bi})(\mu\text{-H})_3$ (eq 2).⁵ Compound **2** will add only 2 equiv of HSnPh_3 to yield compound **3**. It is possible that the bridging $\text{Au}(\text{NHC})$ group with the bulky NHC ligand inhibits a third addition of HSnPh_3 by producing a blocking effect proximate to the third iridium atom. Finally, we observed that H_2O can facilitate cleavage of the phenyl groups from the SnPh_3 ligands in **3** presumably with the formation of some benzene and the formation of an OH group bridging the two tin atoms to yield the compound **4**. The oxygen-bridged linking of the tin ligands could lead to the design and synthesis of an interesting new family of chelating ligands in polynuclear metal complexes in the future.

■ ASSOCIATED CONTENT

Supporting Information

The Supporting Information is available free of charge on the ACS Publications website at DOI: 10.1021/acs.inorgchem.5b01261.

Details of the molecular orbital calculations of compounds **2–4** (PDF)

CIF files for structural analysis of compounds **2–4** (CIF)

■ AUTHOR INFORMATION

Corresponding Author

*E-mail: Adamsrd@mailbox.sc.edu.

Notes

The authors declare no competing financial interest.

■ ACKNOWLEDGMENTS

This research was supported by the U.S. National Science Foundation (Grants CHE-1111496 and CHE-1464596).

■ REFERENCES

- (1) (a) Grasselli, R. K. *Catal. Today* **2014**, 238, 10–27. (b) Grasselli, R. K. *Top. Catal.* **2002**, 21, 79–88. (c) Grasselli, R. K. *Handbook of Heterogeneous Catalysis*; Ertl, G., Knozinger, H., Weitkamp, J., Eds.; VCH Publishers: Weinheim, Germany, 1997; Vol. 5, pp 2302–2326. (d) Grasselli, R. K. *Catal. Today* **2005**, 99, 23–31. (e) Goddard, W. A., III; Chenoweth, K.; Pudar, S.; van Duin, A. C. T.; Cheng, M.-J. *Top. Catal.* **2008**, 50, 2–18. (f) Jang, Y. H.; Goddard, W. A., III *J. Phys. Chem. B* **2002**, 106, 5997–6013.
- (2) Adams, R. D.; Chen, M.; Elpitiya, G.; Potter, M. E.; Raja, R. *ACS Catal.* **2013**, 3, 3106–3110.
- (3) (a) Yamazoe, S.; Koyasu, K.; Tsukuda, T. *Acc. Chem. Res.* **2014**, 47, 816–824. (b) Miyamura, H.; Matsubara, R.; Kobayashi, S. *Chem. Commun.* **2008**, 2031–2033. (c) Hutchings, G. J.; Kiely, C. J. *Acc. Chem. Res.* **2013**, 46, 1759–1772. (d) Hutchings, G. J. *Catal. Today* **2014**, 238, 69–73. (e) Zhang, Y.; Cui, X.; Shi, F.; Deng, Y. *Chem. Rev.* **2012**, 112, 2467–2505. (f) Hutchings, G. J. *Chem. Commun.* **2008**, 1148–1164. (g) Lopez-Sanchez, J. A.; Dimitratos, N.; Glanville, N.; Kesavan, L.; Hammond, C.; Edwards, J. K.; Carley, A. F.; Kiely, C. J.; Hutchings, G. J. *Appl. Catal., A* **2011**, 391, 400–406. (h) Enache, D. I.; Edwards, J. K.; Landon, P.; Solsona-Espriu, B.; Carley, A. F.; Herzing, A. A.; Watanabe, M.; Kiely, C. J.; Knight, D. W.; Hutchings, G. J. *Science* **2006**, 311, 362–365. (i) Miedziak, P.; Sankar, M.; Dimitratos, M.; Lopez-Sanchez, J. A.; Carley, A. F.; Knight, D. W.; Taylor, S. H.; Kiely, C. J.; Hutchings, G. J. *Catal. Today* **2011**, 164, 315–319. (j) Wang, R.; Wu, Z.; Chen, C.; Qin, Z.; Zhu, H.; Wang, G.; Wang, H.; Wu, C.; Dong, W.; Fan, W.; Wang, J. *Chem. Commun.* **2013**, 49, 8250–8252.
- (4) (a) Holt, M. S.; Wilson, W. L.; Nelson, J. H. *Chem. Rev.* **1989**, 89, 11–49. (b) Burch, R.; Garla, L. C. *J. Catal.* **1981**, 71, 360–372. (c) Park, Y.-K.; Ribeiro, F. H.; Somorjai, G. A. *J. Catal.* **1998**, 178, 66–75. (d) Jerdev, D. I.; Olivas, A.; Koel, B. E. *J. Catal.* **2002**, 205, 278–288. (e) Adams, R. D.; Trufan, E. *Philos. Trans. R. Soc., A* **2010**, 368, 1473–1493. (f) Meurig Thomas, J.; Adams, R. D.; Boswell, E. M.; Captain, B.; Gronbeck, H.; Raja, R. *Faraday Discuss.* **2008**, 138, 301–315. (g) Hungria, A. B.; Raja, R.; Adams, R. D.; Captain, B.; Thomas, J. M.; Midgley, P. A.; Golovko, V.; Johnson, B. F. G. *Angew. Chem., Int. Ed.* **2006**, 45, 4782–4785. (h) Adams, R. D.; Boswell, E. M.; Captain, B.; Hungria, A. B.; Midgley, P. A.; Raja, R.; Thomas, J. M. *Angew. Chem., Int. Ed.* **2007**, 46, 8182–8185. (i) Adams, R. D.; Blom, D. A.; Captain, B.; Raja, R.; Thomas, J. M.; Trufan, E. *Langmuir* **2008**, 24, 9223–9226. (j) Das, D.; Mohapatra, S. S.; Roy, S. *Chem. Soc. Rev.* **2015**, 44, 3666–3690.
- (5) Adams, R. D.; Chen, M.; Elpitiya, G.; Zhang, Q. *Organometallics* **2012**, 31, 7264–7271.
- (6) Adams, R. D.; Chen, M. *Organometallics* **2012**, 31, 6457–6465.
- (7) (a) Adams, R. D.; Rassolov, V.; Zhang, Q. *Organometallics* **2013**, 32, 6368–6378. (b) Adams, R. D.; Rassolov, V.; Zhang, Q. *Organometallics* **2013**, 32, 1587–1590.
- (8) Adams, R. D.; Rassolov, V.; Wong, Y. O. *Angew. Chem., Int. Ed.* **2014**, 53, 11006–11009.
- (9) Hashmi, A. S. K.; Ramamurthi, T. D.; Rominger, F. J. *Organomet. Chem.* **2009**, 694, 592–597.
- (10) Garlaschelli, L.; Della Pergola, R.; Martinengo, S.; Ellis, J. E. *Inorg. Synth.* **1990**, 28, 211–215.
- (11) Kruppa, W.; Bläser, D.; Boese, R.; Schmid, G. Z. *Naturforsch., B: J. Chem. Sci.* **1982**, 37, 209–213.
- (12) Gaillard, S.; Slawin, A. M. Z.; Nolan, S. P. *Chem. Commun.* **2010**, 46, 2742–2744.
- (13) SAINT+, version 6.2a; Bruker Analytical X-ray Systems Inc.: Madison, WI, 2001.
- (14) Sheldrick, G. M. *SHELXTL*, version 6.1; Bruker Analytical X-ray Systems Inc.: Madison, WI, 1997.
- (15) *ADF, SCM Theoretical Chemistry*; Vrije Universiteit: Amsterdam, The Netherlands, 2013; <http://www.scm.com>.

- (16) Perdew, J. P.; Ruzsinszky, A.; Csonka, G. I.; Vydrov, O. A.; Scuseria, G. E.; Constantin, L. A.; Zhou, X.; Burke, K. *Phys. Rev. Lett.* **2008**, *100*, 136406.
- (17) (a) Bader, R. F. W. *Atoms in Molecules: A Quantum Theory*; Clarendon Press: Oxford, U.K., 1990. (b) Cortés-Guzmán, F.; Bader, R. F. W. *Coord. Chem. Rev.* **2005**, *249*, 633–662.
- (18) Keith, T. A. *AIMAll*, version 12.11.09; TK Gristmill Software: Overland Park, KS, 2012; aim.tkgristmill.com.
- (19) Adams, R. D.; Chen, M.; Yang, X. *Organometallics* **2012**, *31*, 3588–3598.
- (20) Fernández, E. J.; Laguna, A.; López-de-Luzuriaga, J. M.; Monge, M.; Nema, M.; Olmos, M. E.; Pérez, J.; Silvestru, C. *Chem. Commun.* **2007**, 571–573.
- (21) Lin, T.-P.; Ke, I.-S.; Gabbaï, F. P. *Angew. Chem., Int. Ed.* **2012**, *51*, 4985–4988.
- (22) Tschersich, C.; Limberg, C.; Roggan, S.; Herwig, C.; Ernsting, N.; Kovalenko, S.; Mebs, S. *Angew. Chem., Int. Ed.* **2012**, *51*, 4989–4992.
- (23) Adams, R. D.; Chen, M. *Organometallics* **2011**, *30*, 5867–5872.
- (24) Silvestru, C.; Breunig, H. J.; Althaus, H. *Chem. Rev.* **1999**, *99*, 3277–3327.
- (25) Auer, A. A.; Mansfeld, D.; Nolde, C.; Schneider, W.; Schurmann, M.; Mehring, M. *Organometallics* **2009**, *28*, 5405–5411.
- (26) Stavila, V.; Dikarev, E. V. *J. Organomet. Chem.* **2009**, *694*, 2956–2964.
- (27) Adams, R. D.; Captain, B.; Smith, J. L., Jr.; Hall, M. B.; Beddie, C. L.; Webster, C. E. *Inorg. Chem.* **2004**, *43*, 7576–7578.
- (28) (a) Bau, R.; Drabnis, M. H. *Inorg. Chim. Acta* **1997**, *259*, 27–50. (b) Teller, R. G.; Bau, R. *Struct. Bonding* **1981**, *41*, 1–82.
- (29) Alvarez, M. A.; Alvarez, M. P.; Carreño, R.; Ruiz, M. A.; Bois, C. J. *Organomet. Chem.* **2011**, *696*, 1736–1748.
- (30) Adams, R. D.; Captain, B.; Hollandsworth, C. B.; Johansson, M.; Smith, J. L., Jr. *Organometallics* **2006**, *25*, 3848–3855.